The Response of Cyclic Electron Flow around Photosystem I to Changes in Photorespiration and Nitrate Assimilation[1][W][OPEN]

Berkley J. Walker[2], Deserah D. Strand, David M. Kramer, and Asaph B. Cousins*

Molecular Plant Sciences (B.J.W., A.B.C.) and School of Biological Sciences (A.B.C.), Washington State University, Pullman, Washington 99164; and Biochemistry and Molecular Biology, Michigan State University, East Lansing, Michigan 48824 (D.D.S., D.M.K.)

ORCID ID: 0000-0001-5932-6468 (B.J.W.).

Photosynthesis captures light energy to produce ATP and NADPH. These molecules are consumed in the conversion of CO_2 to sugar, photorespiration, and NO_3^- assimilation. The production and consumption of ATP and NADPH must be balanced to prevent photoinhibition or photodamage. This balancing may occur via cyclic electron flow around photosystem I (CEF), which increases ATP/NADPH production during photosynthetic electron transport; however, it is not clear under what conditions CEF changes with ATP/NADPH demand. Measurements of chlorophyll fluorescence and dark interval relaxation kinetics were used to determine the contribution of CEF in balancing ATP/NADPH in hydroponically grown Arabidopsis (*Arabidopsis thaliana*) supplied different forms of nitrogen (nitrate versus ammonium) under changes in atmospheric CO_2 and oxygen. Measurements of CEF were made under low and high light and compared with ATP/NADPH demand estimated from CO_2 gas exchange. Under low light, contributions of CEF did not shift despite an up to 17% change in modeled ATP/NADPH demand. Under high light, CEF increased under photorespiratory conditions (high oxygen and low CO_2), consistent with a primary role in energy balancing. However, nitrogen form had little impact on rates of CEF under high or low light. We conclude that, according to modeled ATP/NADPH demand, CEF responded to energy demand under high light but not low light. These findings suggest that other mechanisms, such as the malate valve and the Mehler reaction, were able to maintain energy balance when electron flow was low but that CEF was required under higher flow.

Photosynthesis must balance both the amount of energy harvested by the light reactions and how it is stored to match metabolic demands. Light energy is harvested by the photosynthetic antenna complexes and stored by the electron and proton transfer complexes as ATP and NADPH. It is used primarily to meet the energy demands for assimilating carbon (from CO_2) and nitrogen (from NO_3^- and NH_4^+; Keeling et al., 1976; Edwards and Walker, 1983; Miller et al., 2007). These processes require different ratios of ATP and NADPH, requiring a finely balanced output of energy in these forms. For example, if ATP were to be consumed at a greater rate than NADPH, electron transport would rapidly become limiting by the lack of $NADP^+$, decreasing rates of proton translocation and ATP regeneration. Alternatively, if NADPH were consumed faster than ATP, proton translocation through ATP synthase would be reduced due to limiting ADP and the difference in pH between lumen and stroma would increase, restricting plastoquinol oxidation at the cytochrome b_6f complex and initiating nonphotochemical quenching (Kanazawa and Kramer, 2002). The stoichiometric balancing of ATP and NADPH must occur rapidly, because pool sizes of ATP and NADPH are relatively small and fluxes through primary metabolism are large (Noctor and Foyer, 2000; Avenson et al., 2005; Cruz et al., 2005; Amthor, 2010).

The balancing of ATP and NADPH supply is further complicated by the rigid nature of linear electron flow (LEF). In LEF, electrons are transferred from water to $NADP^+$, oxidizing water to oxygen and reducing $NADP^+$ to NADPH. This electron transfer is coupled to proton translocation and generates a proton motive force, which powers the regeneration of ATP. The stoichiometry of ATP/NADPH produced by these reactions is thought to be 1.29 based on the ratio of proton pumping and the requirement for ATP synthase in the thylakoid (Sacksteder et al., 2000; Seelert et al., 2000). However, under ambient CO_2, oxygen, and temperature, the ATP/NADPH required by CO_2 fixation, photorespiration, and NO_3^- assimilation is approximately 1.6 (Edwards and Walker,

[1] This work was supported by the National Science Foundation (grant nos. 0842182 and 0923562 to A.B.C.), by the Achievement Reward for College Scientists Seattle chapter (fellowship to B.J.K.), and by the Division of Chemical Sciences, Geosciences, and Biosciences, Office of Basic Energy Sciences, Department of Energy (grant nos. DE–FG02–04ERl5559 to D.M.K. and D.D.S. and DE–FG02–09ER16062 to A.B.C.).

[2] Present address: Global Change and Photosynthesis Research Unit, U.S. Department of Agriculture Agricultural Research Service, Institute of Genomic Biology, University of Illinois, Urbana, IL 61801.

* Address correspondence to acousins@wsu.edu.

The author responsible for distribution of materials integral to the findings presented in this article in accordance with the policy described in the Instructions for Authors (www.plantphysiol.org) is: Asaph B. Cousins (acousins@wsu.edu).

[W] The online version of this article contains Web-only data.

[OPEN] Articles can be viewed online without a subscription.

www.plantphysiol.org/cgi/doi/10.1104/pp.114.238238

 © 2014 American Society of Plant Biologists. All Rights Reserved.

1983). The ATP/NADPH demand from central metabolism changes significantly from 1.6 if the ratio of CO_2 or oxygen changes, driving different rates of photosynthesis and photorespiration (see "Theory"). Such changes in energy demand require a flexible mechanism to balance ATP/NADPH that responds to environmental conditions.

The difference between ATP/NADPH supply from LEF and demand from primary metabolism could be balanced via cyclic electron flow around PSI (CEF; Avenson et al., 2005; Shikanai, 2007; Joliot and Johnson, 2011; Kramer and Evans, 2011). During CEF, electrons from either NADPH or ferredoxin are cycled around PSI into the plastoquinone pool and regenerate ATP without reducing $NADP^+$ (Golbeck et al., 2006). Therefore, CEF has been suggested to be important for optimal photosynthesis and plant growth, but its physiological role in energy balancing is not clear (Munekage et al., 2002, 2004; Livingston et al., 2010). For example, there was no shift in CEF in Arabidopsis (*Arabidopsis thaliana*) measured under low light (less than 300 μmol m^{-2} s^{-1}) and different oxygen partial pressures, which would significantly change the ATP/NADPH demand of primary metabolism (Avenson et al., 2005). Similar results were seen under low light in leaves of barley (*Hordeum vulgare*) and *Hedera helix* (Genty et al., 1990). While CEF did not shift with energy demand in steady-state photosynthesis under low light, it did increase with photorespiration as expected at high light (Miyake et al., 2004, 2005). These observations could be explained if CEF becomes more important for energy balancing under high irradiances when other mechanisms become saturated.

To determine under which conditions CEF responded to ATP/NADPH demand, we used biochemical models of leaf CO_2 fixation to model ATP and NADPH demand under a variety of conditions (see "Theory"). We then used in vivo spectroscopy to measure the relative response of CEF to modeled ATP/NADPH demand from CO_2 fixation and NO_3^- assimilation in hydroponically grown Arabidopsis. Our findings indicate that CEF responded to modeled ATP/NADPH demand under high light but not under low light or nitrate availability.

THEORY

The ATP and NADPH demand from primary metabolism can be determined from the energy requirements of CO_2 assimilation, photorespiration, and NO_3^- assimilation (Noctor and Foyer, 1998, 2000). The assimilation of CO_2 is the largest energy sink in an illuminated leaf and requires three ATP and two NADPH for the reduction of CO_2 and the regeneration of substrates in the Calvin cycle (Benson and Calvin, 1950; Edwards and Walker, 1983; Noctor and Foyer, 2000). Photorespiration is the second largest energy sink in C_3 species and is initiated when Rubisco reacts with oxygen, requiring 3.5 ATP and two NADPH (Sharkey, 1988; Bauwe et al., 2010). Finally, NO_3^- assimilation is typically the third largest process impacting ATP/NADPH demand and primarily occurs in the leaves of many plants, including Arabidopsis (Noctor and Foyer, 1998). The assimilation of NO_3^- has a much lower ATP/NADPH requirement (one ATP and five NADPH reducing equivalents) and can have a significant effect on energy demand, even though the rates are typically lower than the rates of CO_2 fixation and photorespiration (Smirnoff and Stewart, 1985; Crawford, 1995).

The Farquhar, von Caemmerer, and Berry model of net CO_2 assimilation (A_{net}) can be used to quantify the rates of Calvin cycle and photorespiration:

$$A_{net} = v_c - \alpha v_o - R_d \quad (1)$$

where A_{net} is determined from CO_2 gain through Rubisco carboxylation (v_c) and CO_2 loss following Rubisco oxygenation (v_o) and day respiration (R_d). Photorespiratory loss of CO_2 is calculated from the ratio of CO_2 release per v_o (α), typically assumed to be 0.5. The Michaelis-Menten model for competitive inhibition determines v_c and v_o using carbon (C) and oxygen (O), the K_m values for reaction with CO_2 (K_c) and oxygen (K_o), and maximum rates for reaction with CO_2 (V_{cmax}) and oxygen (V_{omax}) for v_c assuming inhibition by O as in:

$$v_c = \frac{V_{cmax} C}{C + K_c\left(1 + \frac{O}{K_o}\right)} \quad (2)$$

or with respect to v_o inhibited by C as in:

$$v_o = \frac{V_{omax} O}{O + K_o\left(1 + \frac{C}{K_c}\right)} \quad (3)$$

Equations 2 and 3 can be combined with Equation 1 to produce a model of photosynthesis under Rubisco limitation and, through further derivation (Farquhar et al., 1980; von Caemmerer and Farquhar, 1981; von Caemmerer, 2000), produces:

$$A_{net} = \frac{V_{cmax}(C - \Gamma^*)}{C + K_c\left(1 + \frac{O}{K_o}\right)} \quad (4)$$

where Γ^* is the CO_2 compensation point in the absence of day respiration represented by:

$$\Gamma^* = \frac{\alpha V_{omax} K_c}{V_{cmax} K_o} \quad (5)$$

Γ^* can be combined with the electron (e^-) demand for NADPH and Equation 1 to determine maximum A_{net} for a given rate of electron transport, J (von Caemmerer, 2000):

$$A_{net} = \frac{(C - \Gamma^*)J}{\left(4C + 4\frac{\Gamma^*}{\alpha}\right)} - R_d \quad (6)$$

The total energy demand for ATP and NADPH to support v_c, v_o, and NO_3^- assimilation (v_n) can be determined from:

$$v_{NADPH} = 2v_c + 2v_o + 5v_n \quad (7)$$

and

$$v_{ATP} = 3v_c + 3.5v_o + v_n \quad (8)$$

where v_{NADPH} and v_{ATP} are the rates of total demand for NADPH and ATP.

Furthermore, the total amount of electron transport required for v_c and v_o (J_g) can be calculated from measured rates of A_{net} by rearrangement of Equation 6 (Ruuska et al., 2000) to produce:

$$J_g = \frac{(A_{net} + R_d)\left(4C + 4\frac{\Gamma^*}{\alpha}\right)}{(C - \Gamma^*)} \quad (9)$$

and for ATP demand as:

$$v_{ATP} - v_n = \frac{(A_{net} + R_d)\left(3C + 3.5\frac{\Gamma^*}{\alpha}\right)}{(C - \Gamma^*)} \quad (10)$$

Rates of CEF necessary to balance ATP and NADPH are determined by subtracting the amount of ATP produced by LEF from v_{ATP} according to:

$$\text{ATP needed from CEF} = v_{ATP} - v_{NADPH}\frac{1.29\ \text{ATP}}{\text{NADPH}} \quad (11)$$

which is converted to electron demand assuming CEF pumping of 2 H^+/e^- and an ATP synthase requirement of 4.7 H^+/ATP:

$$e^- \text{ from CEF} = \left(v_{ATP} - v_{NADPH}\frac{1.29\ \text{ATP}}{\text{NADPH}}\right)\frac{4.7H^+}{\text{ATP}}\frac{e^-}{2H^+} \quad (12)$$

Total demand for CEF can be simplified from Equation 12 as a percentage of LEF as:

$$\%\text{CEF} = \frac{(1.18v_{ATP} - 1.52v_{NADPH})}{v_{NADPH}} * 100 \quad (13)$$

which predicts CEF demand using Equations 2 and 3 or 9 and 10.

RESULTS

CO_2 Exchange and Leaf Absorbance under NO_3^- and NH_4^+ Feeding

To parameterize CO_2 exchange models for calculating predicted rates of CEF (see "Theory"), Γ^*, R_d, and V_{cmax} were determined under NO_3^- and NH_4^+ feeding. Nitrogen form had no significant effect on Γ^* (4.1 ± 0.3 and 3.9 ± 0.3 Pa CO_2 for NO_3^-- and NH_4-fed plants) or R_d (0.41 ± 0.03 and 0.57 ± 0.10 μmol CO_2 m^{-2} s^{-1} for NO_3^-- and NH_4-fed plants; Table I; Student's t test $P > 0.05$). Rates of V_{cmax} decreased with measurement photosynthetic photon flux density (PPFD) but were not significantly different between nitrogen treatments (Table I; Student's t test $P > 0.05$). Photosynthetic rates near ambient CO_2 (37 Pa) and saturating PPFD (1,000 μmol m^{-2} s^{-1}) were also similar between nitrogen-feeding treatments (Table I), and there was no difference in photosynthetic rates under any other PPFD (data not shown). Leaf absorbance measured with an integrating sphere for calculating LEF was 0.860 ± 0.006.

Modeled Cyclic Electron Flow under Low-Light Conditions

The rate at which CEF would need to operate to match ATP and NADPH production to demand was estimated for several partial pressures of CO_2, oxygen, and nitrogen form using nitrogen form-specific values of Γ^*, R_d, and V_{cmax} (Table II). Predicted rates of CEF were largest under high photorespiration (15 Pa of CO_2 and 37 kPa of oxygen) and smallest under low photorespiration (200 Pa of CO_2 and 2 kPa of oxygen)

Table I. *Parameters from Laisk curves used to model rates of cyclic electron flow*

CO_2 assimilation rates measured at subsaturating light intensities (Laisk curves) were used to determine Γ^*, rates of R_d, and CO_2 assimilation at 36 Pa of CO_2 and 1,000 μmol m^{-2} s^{-1} PPFD. V_{cmax} was determined from the linear portions of photosynthetic CO_2 response curves measured under 1,000, 377, 210, 120, 66, and 24 μmol m^{-2} s^{-1} PPFD. Measurements were made in hydroponically grown plants starved of all nitrogen for 24 h and then fed either NO_3^- or NH_4^+ as the sole nitrogen form. Values shown are averages of five separate plants ± SE. There were no significant differences in any values as determined using Student's t test with $P < 0.05$.

Parameter	NO_3^- Feeding	NH_4 Feeding
Γ^* (Pa of CO_2)	4.11 ± 0.25	3.91 ± 0.25
R_d (μmol CO_2 m^{-2} s^{-1})	0.41 ± 0.03	0.57 ± 0.10
CO_2 assimilation at 36 Pa of CO_2 (μmol CO_2 m^{-2} s^{-1})	9.6 ± 0.8	9.9 ± 0.9
V_{cmax} (μmol CO_2 m^{-2} s^{-1})		
1,000 μmol m^{-2} s^{-1} PPFD	31.6 ± 3.1	32.4 ± 3.3
377 μmol m^{-2} s^{-1} PPFD	27.3 ± 2.1	28.7 ± 3.2
210 μmol m^{-2} s^{-1} PPFD	23.3 ± 1.9	25.5 ± 1.6
120 μmol m^{-2} s^{-1} PPFD	14.4 ± 1.5	15.2 ± 1.1
66 μmol m^{-2} s^{-1} PPFD	7.6 ± 0.6	9.4 ± 1.2
24 μmol m^{-2} s^{-1} PPFD	1.8 ± 0.5	2.2 ± 0.5

regardless of the assumed H^+/ATP requirement for ATP synthase. NO_3^- assimilation decreased ATP/NADPH demand within each CO_2 and oxygen condition. The most extreme differences in hypothetical CEF demand were between high photorespiratory conditions without NO_3^- assimilation and low photorespiratory conditions with NO_3^- assimilation. The modeled difference in CEF between these conditions was 17%, assuming an H^+/ATP requirement of 4.7 H^+/ATP.

Comparison of Rates of Proton Flux with Linear Electron Flow under Low Light

Proton pumping during LEF produces a fixed relationship between proton flux through the thylakoid membrane (v_{H+}) and LEF. Because CEF increases the amount of v_{H+} relative to LEF, increases in CEF correlate to increases in the slope between v_{H+} and LEF. We observed no major shifts in plots of v_{H+} against LEF under any of the conditions modeled in Table II (Fig. 1A). There was, however, a slight decrease in the relationship of v_{H+}/LEF from conditions of lowest ATP/NADPH demand (205 Pa of CO_2, 2 kPa of oxygen, NO_3^-) to highest ATP/NADPH demand (14 Pa of CO_2, 37 kPa of oxygen, NH_4^+; Fig. 1B). This shift was in the opposite direction from that expected based on modeled CEF demand (Table II; modeled lines are shown in Fig 1B).

Rates of CEF under High Light and Variable CO_2

Modeling suggested that ATP/NADPH demand should increase at low CO_2 partial pressures under ambient oxygen (20 kPa) and increase rates of CEF both with and without NO_3^- assimilation (Fig. 2A, lines). Nitrate assimilation was predicted to decrease overall rates of necessary CEF by approximately 4% at high CO_2 (90 Pa) to approximately 13% at low CO_2 (6 Pa). Under low oxygen (2 kPa; Fig. 2B, lines), CEF was expected to increase with low CO_2 with no NO_3^- assimilation (Fig. 2B, dotted line), but CEF is modeled to decrease at low CO_2 when NO_3^- assimilation is present (Fig. 2B, solid line).

At ambient oxygen, measured CEF estimated by the v_{H+}/LEF was similar to modeled predictions of CEF in general but not in absolute differences between nitrogen form treatments (Fig. 2A). Specifically, the v_{H+}/LEF in both the NO_3^-- and NH_4^+-fed treatments gradually increased with decreasing CO_2 as the modeled trend would suggest, but there was no difference between nitrogen treatments despite a predicted 4% to 13% decrease when NO_3^- assimilation was absent.

At low oxygen, the ratio v_{H+}/LEF increased sharply as the CO_2 availability decreased but started at a similar value as ambient oxygen under high CO_2 in both the NO_3^-- and NH_4^+-fed treatments (Fig. 2B). This response was similar to the general trend of CEF predicted from ATP/NADPH demand when NO_3^- assimilation was absent but differed from what was expected when NO_3^- assimilation was present.

ANOVA revealed a significant CO_2 effect on the ratio v_{H+}/LEF and an interaction between CO_2 and oxygen (Table III), but no statistically significant difference or interaction involving nitrogen form was seen at the $P < 0.05$ level.

Linear Electron Flow and Comparisons of NADPH Supply and Demand

Rates of LEF measured using the multiphase flash protocol of the LI-COR 6400 compared well with the rates measured on the custom-built IDEASpec spectrophotometer and fluorometer (Hall et al., 2012), producing a 1:1 ratio at all measured CO_2 partial pressures and nitrogen form feedings (Supplemental Fig. S1). This indicates that partial saturation of PSII centers did not interfere with our results. Rates of J_g determined from gas exchange according to Equation 9 were strongly correlated with rates of LEF (Fig. 3). Under various PPFD values at ambient oxygen (Fig. 3A) and CO_2 partial pressures under low oxygen (Fig. 3C), the relationship between J_g and LEF matched nearly 1:1. When J_g was varied through changes in CO_2 partial pressure under ambient oxygen, the relationship between J_g and LEF matched a 1:1 ratio under all conditions except for the point corresponding to the lowest CO_2, where rates of LEF were higher than J_g (Fig. 3B).

Table II. *Estimated cyclic electron flow under a variety of oxygen, CO_2, and nitrogen availabilities*

Cyclic electron flow is shown as a percentage of LEF required to balance the ATP/NADPH requirements of photosynthesis, photorespiration, and NO_3^- assimilation under various oxygen, CO_2, and NO_3^- conditions. Determination of LEF was made using Equations 2, 3, and 7 with kinetics from Walker et al. (2013). Calculations were made using H^+/ATP of both 4 and 4.7. C_c, CO_2 partial pressure within the chloroplast.

C_c	Oxygen	v_c	v_o	Nitrate	ATP/NADPH Demand	LEF	Cyclic 4.7 H^+/ATP	Cyclic 4 H^+/ATP
Pa	*kPa*			*μmol m^{-2} s^{-1}*			*%*	
200	1.8	21.9	0.1	0.00	1.50	88	25	21
200	1.8	21.9	0.1	0.17	1.48	90	22	19
20	19.0	6.7	2.5	0.00	1.57	37	33	28
20	19.0	6.7	2.5	0.17	1.51	38	26	22
15	36.8	3.9	3.7	0.00	1.62	30	39	33
15	36.8	3.9	3.7	0.17	1.55	32	30	26

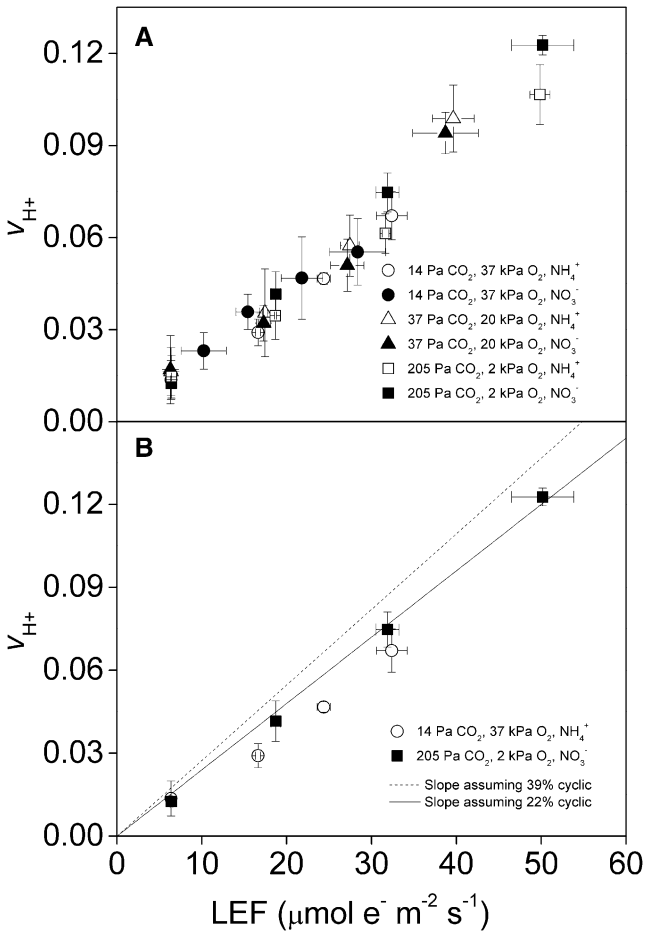

Figure 1. Response of CEF to changes in ATP/NADPH demand under subsaturating PPFD. CEF was measured from the relationship of LEF (μmol e^- m^{-2} s^{-1}) to the rate of v_{H+} in relative units. The subsaturating light intensities ranged from 34 to 377 μmol m^{-2} s^{-1} PPFD. v_{H+} was determined spectroscopically from the dark relaxation of the ECS and LEF was determined using chlorophyll fluorescence. CEF was measured under various partial pressures of CO_2 and oxygen (14 Pa of CO_2 and 37 kPa of oxygen [circles], 37 Pa of CO_2 and 20 kPa of oxygen [triangles], and 205 Pa of CO_2 and 2 kPa of oxygen [squares]) and hydroponically supplied nitrogen (NH_4^+ [white symbols] or NO_3^- [black symbols]). All treatments (A) and treatments of the largest ATP/NADPH demand differences (B) are shown with modeled lines representing expected slopes assuming 24% CEF (solid line) and 39% CEF (dashed line), as presented in Table II. Values shown are averages of measurements from five separate plants ± SE.

DISCUSSION

The aim of this work was to test if CEF responded to the ATP/NADPH demand estimated using leaf models of CO_2 exchange and nitrate metabolism. This relationship was determined under both high and low light. Under low light, the relationship v_{H+}/LEF did not increase with the modeled demand for ATP/NADPH (Fig. 1A). For example, there was a slight decrease in v_{H+}/LEF between conditions of lowest (205 Pa of CO_2, 2 kPa of oxygen, NO_3^-) and highest (14 Pa of CO_2, 37 kPa of oxygen, NH_4^+) ATP/NADPH demand when CEF would be expected to increase if it were responding to energy demand (Fig. 1B; Table II). However, under high light, the ratio v_{H+}/LEF responded to CO_2 as predicted if CEF was the primary contributor to balancing ATP/NADPH production. This was demonstrated by the gradual increase in CEF under ambient oxygen as CO_2 decreased and the sharp increase in CEF at low CO_2 when photorespiration was minimized with 2 kPa of oxygen (Fig. 2). These changes in CEF matched the trend predicted from estimated ATP/NADPH demand assuming that CEF was the primary mechanism in energy balancing.

These findings are consistent with previous work done in separate low- and high-light studies. For example, there was no change in CEF when measured under PPFD irradiances below 200 μmol m^{-2} s^{-1} in

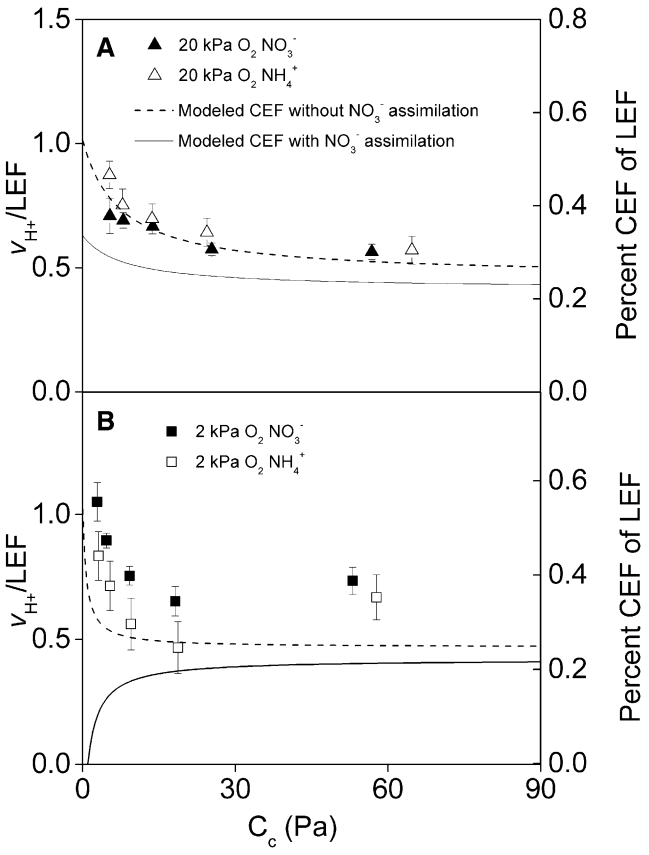

Figure 2. Response of CEF to changes in ATP/NADPH demand under saturating PPFD. CEF was measured from the relationship of LEF (μmol e^- m^{-2} s^{-2}) to the rate of v_{H+} in relative units measured as in Figure 1. Plants were measured under saturating PPFD (1,000 μmol m^{-2} s^{-1}) and various CO_2 partial pressures. Chloroplastic CO_2 partial pressure (C_c) was determined from separate measurements of gas exchange made under identical conditions. Plants were measured under ambient (20 kPa) oxygen (triangles) and low (2 kPa) oxygen (squares) and under hydroponic NO_3^- feeding (black symbols) or NH_4^+ feeding (white symbols). Values shown are averages of three to four separate plants ± SE. Modeled lines represent the predicted demand for CEF estimated using Equations 2 and 3 to balance ATP/NADPH supply with demand assuming 4.7 H^+/ATP without NO_3^- assimilation (dotted lines) or with NO_3^- assimilation (solid lines).

Table III. *ANOVA results from high-light LEF and v_{H+} plots*

Results are shown from ANOVA of the ratio v_{H+}/LEF against the effects of oxygen, CO_2, and either NH_4^+ or NO_3^- treatment (N form).

Effect	Numerator Degrees of Freedom	Denominator Degrees of Freedom	*F* Value	*P* Value
Oxygen	1	13.7	0.68	0.4247
CO_2	4	34.7	76.19	<0.0001
N form	1	13.7	1.68	0.2167
Oxygen × CO_2	4	34.7	7.11	0.0003
Oxygen × N form	1	9.91	4.68	0.0561
CO_2 × N form	4	34.7	0.60	0.6666
CO_2 × oxygen × N form	4	34.7	1.03	0.4073

Arabidopsis exposed to ambient and high photorespiratory conditions (Avenson et al., 2005). However, there were increases in CEF under decreasing CO_2 detected in tobacco (*Nicotiana tabacum*) measured under 1,000 μmol m^{-2} s^{-1} PPFD (Miyake et al., 2005). Additionally, the hypothesis that CEF is most important under saturating but not subsaturating photosynthetic electron flows is supported by mutants lacking key enzymes involved in CEF. For example, mutants lacking both the NADPH- and ferredoxin-dependent pathway of CEF were viable under a reduced PPFD, suggesting that alternative mechanisms can balance ATP/NADPH supply in the absence of CEF (Munekage et al., 2002, 2004).

The response of CEF in this study relied on accurately measured rates of LEF. Rates of LEF were determined from measurements of photochemical efficiency of PSII (Φ_{II}) by a saturating pulse of actinic light (Maxwell and Johnson, 2000). Subsaturating flashes of light used to determine Φ_{II} could result in underestimated LEF rates and might explain increases in v_{H+}/LEF independent from changes in CEF rates. To confirm that LEF was not underestimated during measurements of v_{H+}/LEF, the LEF determined from the spectroscope was compared with that from the fluorimeter on the LI-COR 6400XT (6400-40 Leaf Chamber Fluorimeter; Li-Cor Biosciences). The multiphase flash protocol used in the LI-COR 6400XT produces saturating values of chlorophyll fluorescence even under subsaturating flash intensity to accurately determine Φ_{II} (Loriaux et al., 2013). Values of LEF were similar when measured under identical conditions at ambient and low oxygen using either the spectroscope or the LI-COR multiphase flash (Supplemental Fig. S1), confirming that values of LEF were not underestimated in calculating v_{H+}/LEF.

The absolute rates of CEF necessary to balance ATP/NADPH depend on the proton requirement of chloroplastic ATP synthase (H^+/ATP). The ratio of H^+/ATP is still under debate, with mechanistic models predicting a requirement of 4.7 H^+/ATP but experimental measurements indicating H^+/ATP closer to 4 (Petersen et al., 2012). In this study, the rates of CEF needed to balance ATP/NADPH demand under all conditions were larger assuming a greater proton requirement for ATP synthase (4.7 as compared with 4 H^+/ATP). While a lower proton requirement would decrease the absolute demand for CEF, relative shifts in the relationship v_{H+}/LEF would remain the same. This study also assumed continuous Q cycle activation resulting in two H^+ pumped per e^- through CEF. Lower H^+ per e^- ratios would increase the demand for CEF, but relative predicted shifts would stay the same.

The Impact of Nitrogen Form Treatment

It is interesting that while there were shifts in CEF consistent with estimated ATP/NADPH demand from photorespiration and CO_2 fixation, there were no differences as expected under NO_3^- or NH_4^+ feeding. This observation could be explained if the experimental NO_3^- assimilation rates were lower than what was used for modeling ATP/NAPDH demand. The ATP/NADPH modeling assumed a rate of NO_3^- assimilation of 0.17 μmol m^{-2} s^{-1}, which was measured in plants reared under similar conditions from the same seed stock (A. Gandin, unpublished data). This rate is comparable to NO_3^- assimilation rates measured in other studies of Arabidopsis, which range from approximately 0.07 to 0.6 μmol m^{-2} s^{-1} assuming a dry leaf-specific weight of 40 g m^{-2} to calculate rates on an area basis (Rachmilevitch et al., 2004; Bloom et al., 2010). However, in this study, the nearly 1:1 relationship between LEF and J_g suggests that the majority of reductant produced from LEF went toward CO_2 fixation and photorespiration (Fig. 3). In previous studies, there was also little difference in electron flow between NO_3^- and NH_4^+ feedings in Arabidopsis and wheat (*Triticum aestivum*), which corresponded to lower leaf NO_3^- reductase activity (Cousins and Bloom, 2004; Rachmilevitch et al., 2004). Furthermore, nitrate reductase activity can decrease under lower light intensities, minimizing the impact of nitrate reduction to leaf energy balance under low PPFD (Pilgrim et al., 1993; Lillo and Appenroth, 2001).

Alternatively, the lack of nitrogen form effect on CEF, LEF, and J_g could be explained if reducing power for NO_3^- assimilation did not come directly from the chloroplast. However, most of the energy for NO_3^- assimilation comes from ferredoxin and ATP during the conversion of NO_2^- to Glu in the chloroplast stroma, making transport from the mitochondria unlikely (Lea and Miflin, 1974; Miflin, 1974; Keys et al., 1978).

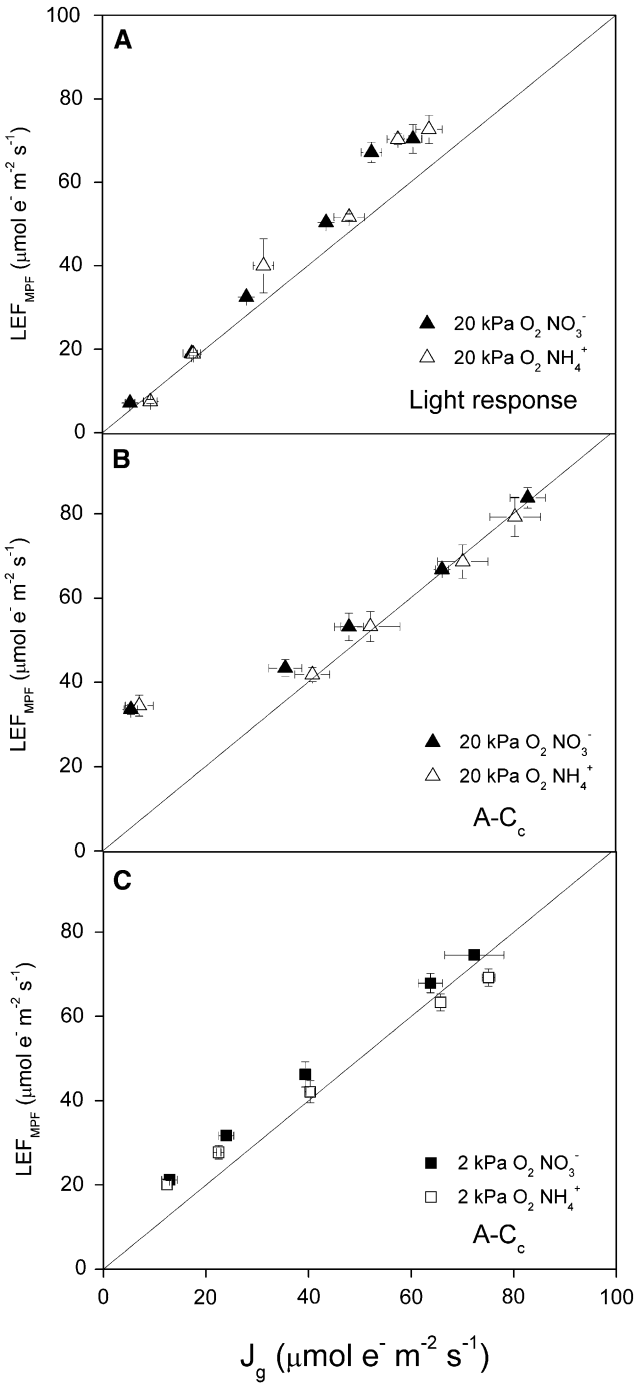

Figure 3. Rates of linear electron flow measured using chlorophyll florescence (LEF_{MPF}) and predicted from gas exchange (J_g) under subsaturating and saturating PPFD. Chlorophyll fluorescence in Arabidopsis was used to calculate rates of LEF_{MPF}. Gas exchange was used to predict LEF using measurements of net CO_2 exchange and biochemical models of photosynthesis (J_g). Both LEF and J_g were measured under hydroponic feeding of NO_3^- (black symbols) or NH_4^+ (white symbols) at either 37 Pa of CO_2 and subsaturating (34–377 μmol m^{-2} s^{-1}) PPFD (A) or in response to CO_2 (A-C_c) under a saturating PPFD of 1,000 μmol m^{-2} s^{-1} at 20 kPa of oxygen (B) or 2 kPa of oxygen (C). The solid lines represent a 1:1 relationship of LEF and J_g. Values shown are averages of three to four separate plants ± SE.

While there were no statistically significant effects of nitrogen form on CEF, the *P* value for the interaction between nitrogen form and oxygen was almost significant under high light ($P = 0.0561$; Table III). If significant, this interaction indicated that, under ambient oxygen partial pressures, CEF decreased with NO_3^- assimilation. Because NO_3^- assimilation decreases the total ATP/NADPH demand, such a response would be expected if CEF was regulated to balance energy supply. In contrast to ambient oxygen, this interaction would also indicate that, at lower oxygen partial pressures, CEF increased with NO_3^- assimilation. This would be unexpected due to the assumption that NO_3^- assimilation decreases ATP/NADPH demand, which would decrease the demand for CEF if it were regulated by energy balancing. However, the impact of NO_3^- assimilation to cellular ATP/NADPH demand could be masked by unaccounted for ATP demand, such as in the transport cost of nitrite transport into the chloroplast.

We also did not observe an effect of nitrogen form on Γ^* and R_d. These parameters were reported to change with nitrogen form availability in hydroponically grown bean (*Phaseolus vulgaris*) due to an increased need for carbon skeletons during NO_3^- assimilation (Guo et al., 2005). This discrepancy between studies also could be due to lower rates of NO_3^- assimilation in Arabidopsis compared with bean.

Energy Balancing under Low and High Light

Taken together, the findings from this and previous studies support the position that different mechanisms coordinate to balance ATP/NADPH supply and demand under low and high light. Under subsaturating irradiances, this balancing could be accomplished through mechanisms such as the malate shuttle, where excess chloroplastic NADPH reduces oxaloacetate to malate, which is transported to the mitochondria and used in mitochondrial electron transport (Scheibe, 2004). This shuttling not only consumes excess NADPH, as suggested in recent work with alternative oxidase mutants (Gandin et al., 2012), but may produce ATP, which could enter the chloroplast via a plastidic ADP/ATP transporter and further increase the ATP/NADPH supply (Neuhaus et al., 1997; Möhlmann et al., 1998). The Mehler reaction also increases ATP/NADPH supply by diverting electrons from $NADP^+$ to reactive oxygen species and ultimately back to water. These electrons generate a proton motive force for ATP regeneration without $NADP^+$ reduction; however, the relevance of the Mehler reaction to steady-state photosynthesis in higher plants is debated and has been suggested to not occur at high enough rates under ambient conditions to fully balance energy production in the chloroplast (Asada, 1999; Badger et al., 2000; Ruuska et al., 2000; Heber, 2002). As irradiance increases, the capacity for these alternative mechanisms could saturate and increase the importance of CEF to modulate ATP/NADPH supply.

CONCLUSION

CEF is proposed to play a role in balancing ATP/NADPH supply with metabolic demand from central carbon and NO_3^- assimilation. However, the data presented here indicated that, under low-light conditions, CEF did not respond to estimated ATP/NADPH demand, suggesting that mechanisms like the malate shuttle and the Mehler reaction participated in energy balancing when electron flow was low. Under high light, CEF corresponded with changes in estimated ATP/NADPH demand at ambient and low oxygen, consistent with CEF becoming a major mechanism for energy balancing when electron flows were high. Furthermore, there was little difference in the impact of NO_3^- and NH_4^+ hydroponic feeding on CEF or rates of electron flow in mature Arabidopsis.

MATERIALS AND METHODS

Hydroponic Setup and Plant Growth

Arabidopsis (*Arabidopsis thaliana*) ecotype Colombia seeds were sown on germination plugs prepared by using a cork borer to cut 4-cm-thick cylinders from rock wool (Grodan) that had been rinsed three times in deionized water to remove residual salt. Approximately 35 germination plugs were placed in a 23-cm^2 container containing a commercial hydroponic solution (Ionic Grow Hard Water; Hydrodynamics International), stratified for 2 d at 4°C, and placed uncovered into a climate-controlled cabinet (Econair Ecological Chambers) under a PPFD of 100 to 150 μmol m^{-2} s^{-1} with day/night cycles of 11/13 h and 23°C/18°C. The solution level was maintained with deionized water and allowed to periodically dry out to minimize algae growth.

After 1 to 2 weeks, seedlings were thinned to one plant per plug and grown for an additional 2 weeks, until roots extended through the rock wool and six true leaves were formed and well developed. Plants in the plugs were then transferred to hollowed green neoprene stoppers (size #5 1/5) and placed in a predrilled Plexiglas sheet covered with aluminum foil on top of a 37-L container containing 25 L of a nutrient solution (Epstein and Bloom, 2004). The hydroponic solution was vigorously bubbled with compressed air and replaced twice weekly. The solution level was maintained so that the aeration caused the solution to splash onto the plug bottoms but not so high that the plugs were constantly submerged in the medium. The solution level was decreased as roots extended into the medium until plants were grown in 10 L of solution after an additional 2 to 3 weeks. Plants were measured between 40 and 50 d after planting, when leaves were large enough for gas-exchange and spectroscopic measurements.

Hydroponic Feeding and Gas Exchange

Before measurements of gas exchange or in vivo spectroscopy, plants were placed for 24 h in a nutrient solution lacking any nitrogen to exhaust active NO_3^- pools within the plant (Rachmilevitch et al., 2004). Subsequently, plants were transferred to a custom-built root cuvette supplied with either NO_3^- or NH_4^+ medium overnight (Rachmilevitch et al., 2004). The cuvette was temperature controlled using a water bath to 25°C and fed aerated solution at a rate of 7 mL min^{-1} using either a peristaltic or Teflon piston pump (Q pump; Fluid Metering). Plants were illuminated with a PPFD of 100 to 150 μmol m^{-2} s^{-1} for at least 1 h prior to each measurement. Gas exchange and chlorophyll fluorescence using a multiphase saturation flash were measured on fully expanded leaves completely filling a 2-cm^2 measuring head (6400-40 Leaf Chamber Fluorometer; Li-Cor Biosciences). The oxygen partial pressure was varied using mass flow controllers (Aalborg) and passed through a humidification flask before entering the LI-COR 6400XT. The band-broadening effects of oxygen on the measuring wavelength were accounted for according to the manufacturer's instructions (LI-COR 6400XT manual version 6).

The Γ^* (x intercept) and R_d (y intercept) were measured using the intercept of photosynthetic CO_2 response (A-C_i) curves measured under subsaturating (1,000, 377, 210, 120, 66, and 24 μmol m^{-2} s^{-1}) PPFD (Laisk, 1977). CO_2 diffusion through the gasket was corrected according to the manufacturer's instructions (LI-COR 6400XT manual version 6), and Γ^* (chloroplastic CO_2 partial pressure of intercept) was calculated from the intercellular partial pressure (C^*) using $\Gamma^* = C^* + R_d/g_m$, where g_m (mesophyll conductance) was 2 mol CO_2 m^{-2} MPa^{-1}, which was the average of several Arabidopsis ecotypes measured under various conditions (Tazoe et al., 2011). The V_{cmax} was determined from the initial slopes of the A-C_i curves for each light intensity using a derivation of the Farquhar, von Caemmerer, and Berry biochemical model for leaf CO_2 exchange (von Caemmerer and Farquhar, 1981). Additional A-C_i curves were measured under saturating (1,000 μmol m^{-2} s^{-1}) PPFD and a wider range of CO_2 partial pressures (92, 36.8, 18.4, 9.2, and 4.6 Pa of CO_2) at both 20 and 2 kPa of oxygen.

In Vivo Spectroscopy

The steady-state v_{H+} was estimated from the dark interval relaxation of the electrochromic shift (ECS) at 520 nm in a custom-built spectroscope described previously on plants receiving the same nitrogen starvation period and feeding regime described above (Sacksteder and Kramer, 2000; Cruz et al., 2005). Because the extent of the ECS signal is proportional to the light-induced proton motive force, a relative value of v_{H+} through the thylakoid in the light was calculated from the maximal drop in the ECS signal (ECS_t) during a 300-ms dark interval and the time constant of the ECS decay (τ_{ECS}): $v_{H+} = ECS_t/\tau_{ECS}$ (Baker, 1996; Kanazawa and Kramer, 2002; Cruz et al., 2005; Baker et al., 2007).

Rates of LEF and other fluorescence parameters were derived from variable chlorophyll *a* fluorescence after 18 min of illumination and during a dark interval of 10 min (Genty et al., 1989; Kramer and Crofts, 1989; Kanazawa and Kramer, 2002). Rates of LEF were calculated from fluorescence yield under steady-state PPFD (f_s) and under a saturating flash (f_m') according to:

$$\mathrm{LEF} = \frac{f_m' - f_s}{f_m'} * \mathrm{Abs}_{\mathrm{leaf}} * \mathrm{fraction}_{\mathrm{PSII}}$$

where Abs_{leaf} and $fraction_{PSII}$ are leaf absorbance and the fraction of light energy capture by PSII as compared with total photosystems. Leaf absorbance was determined from measurements of reflectance and transmittance from five representative leaves using an integrating sphere (Labsphere) according to the manufacturer's instructions. The $fraction_{PSII}$ was assumed to be 0.5.

Measuring atmosphere and feeding regime were introduced to the leaf and plant using an attached LI-COR 6400 with oxygen-mixing system and feeding cuvette as outlined above. For measurements under low light, plants were placed in the conditions outlined in Table II under five subsaturating light intensities (377, 210, 120, 66, and 24 μmol m^{-2} s^{-1}), and relative CEF was determined from shifts in the slope of a plot of v_{H+} versus LEF between conditions. The response of CEF to high light under decreasing CO_2 (92, 36.8, 18.4, 9.2, and 4.6 Pa of CO_2) was measured at 20 and 2 kPa of oxygen under NO_3^- and NH_4^+ feeding. The CO_2 partial pressure within the chloroplast was calculated for Figure 2 from CO_2 gas exchange measured under similar conditions using the LI-COR 6400XT.

Cyclic and Linear Electron Flow Modeling

Rates of CEF sufficient to balance ATP/NADPH demand were estimated using the equations outlined in "Theory." For CEF modeling from v_c and v_o under low light, Equations 2 and 3 were parameterized with the in vivo Rubisco kinetics for Arabidopsis presented previously (Walker et al., 2013) and V_{cmax} calculated from the initial slope of A-C_i curves reported in Table I for 277 μmol m^{-2} s^{-1}. The rate of NO_3^- assimilation was assumed to be 0.17 μmol m^{-2} s^{-1}, as measured in hydroponically grown Arabidopsis grown under similar conditions (A. Gandin, unpublished data). For high-light treatments, rates of CEF were predicted in two ways: (1) from v_c and v_o using Equations 2 and 3, and (2) using Equations 9 and 10 from gas exchange parameterized with Γ^* and R_d for each feeding form.

Statistics

Student's t tests were performed using Statistix 9 (Analytical Software) with significance determined as $P < 0.05$. The repeated-measures ANOVA for high-light data was performed using SAS version 9.2 (SAS Institute). The Kenward-Roger approximation was applied to correct the denominator for degrees of freedom (Arnau et al., 2009).

Supplemental Data

The following materials are available in the online version of this article.

Supplemental Figure S1. Rates of linear electron flow in response to subsaturating light intensities measured using a multiphase flash (LEF_{MPF}) from the LI-COR 6400XT and an in vivo spectroscope (LEF_{spec}).

ACKNOWLEDGMENTS

We thank Robert Zegarac for technical assistance and troubleshooting, Charles Cody for growth space maintenance, and Dr. Anthony Gandin for help with hydroponics optimization.

Received February 19, 2014; accepted March 17, 2014; published March 24, 2014.

LITERATURE CITED

Amthor JS (2010) From sunlight to phytomass: on the potential efficiency of converting solar radiation to phyto-energy. New Phytol **188:** 939–959

Arnau J, Bono R, Vallejo G (2009) Analyzing small samples of repeated measures data with the mixed-model adjusted F test. Commun Statist Simulation Comput **38:** 1083–1103

Asada K (1999) The water-water cycle in chloroplasts: scavenging of active oxygens and dissipation of excess photons. Annu Rev Plant Physiol Plant Mol Biol **50:** 601–639

Avenson TJ, Cruz JA, Kanazawa A, Kramer DM (2005) Regulating the proton budget of higher plant photosynthesis. Proc Natl Acad Sci USA **102:** 9709–9713

Badger MR, von Caemmerer S, Ruuska S, Nakano H (2000) Electron flow to oxygen in higher plants and algae: rates and control of direct photoreduction (Mehler reaction) and Rubisco oxygenase. Philos Trans R Soc Lond B Biol Sci **355:** 1433–1446

Baker NR (1996) Photosynthesis and the Environment, Vol 5. Kluwer Academic Publishers, Dordrecht

Baker NR, Harbinson J, Kramer DM (2007) Determining the limitations and regulation of photosynthetic energy transduction in leaves. Plant Cell Environ **30:** 1107–1125

Bauwe H, Hagemann M, Fernie AR (2010) Photorespiration: players, partners and origin. Trends Plant Sci **15:** 330–336

Benson AA, Calvin M (1950) Carbon dioxide fixation by green plants. Annu Rev Plant Physiol **1:** 25–42

Bloom AJ, Burger M, Rubio Asensio JS, Cousins AB (2010) Carbon dioxide enrichment inhibits nitrate assimilation in wheat and Arabidopsis. Science **328:** 899–903

Cousins AB, Bloom AJ (2004) Oxygen consumption during leaf nitrate assimilation in a C_3 and C_4 plant: the role of mitochondrial respiration. Plant Cell Environ **27:** 1537–1545

Crawford NM (1995) Nitrate: nutrient and signal for plant growth. Plant Cell **7:** 859–868

Cruz JA, Avenson TJ, Kanazawa A, Takizawa K, Edwards GE, Kramer DM (2005) Plasticity in light reactions of photosynthesis for energy production and photoprotection. J Exp Bot **56:** 395–406

Edwards GE, Walker DA (1983) C_3, C_4: Mechanisms, and Cellular and Environmental Regulation, of Photosynthesis. Oxford, London

Epstein E, Bloom AJ (2004) Mineral Nutrition of Plants: Principles & Perspectives, Vol 2. Sinauer, Sunderland, MA

Farquhar GD, von Caemmerer S, Berry JA (1980) A biochemical model of photosynthetic CO_2 assimilation in leaves of C_3 species. Planta **149:** 78–90

Gandin A, Duffes C, Day DA, Cousins AB (2012) The absence of alternative oxidase AOX1A results in altered response of photosynthetic carbon assimilation to increasing CO(2) in Arabidopsis thaliana. Plant Cell Physiol **53:** 1627–1637

Genty B, Briantais JM, Baker NR (1989) The relationship between the quantum yield of photosynthetic electron transport and quenching of chlorophyll fluorescence. Biochim Biophys Acta **990:** 87–92

Genty B, Harbinson J, Baker NR (1990) Relative quantum efficiencies of the two photosystems of leaves in photorespiratory and non-respiratory conditions. Plant Physiol Biochem (Paris) **28:** 1–10

Golbeck J, Joliot P, Joliot A, Johnson G (2006) Cyclic electron transfer around photosystem I. *In* Photosystem I, Vol 24. Springer, Houten, The Netherlands, pp 639–656

Guo S, Schinner K, Sattelmacher B, Hansen UP (2005) Different apparent CO_2 compensation points in nitrate- and ammonium-grown *Phaseolus vulgaris* and the relationship to non-photorespiratory CO_2 evolution. Physiol Plant **123:** 288–301

Hall C, Cruz J, Wood M, Zegarac R, DeMars D, Carpenter J, Kanazawa A, Kramer D (2012) Photosynthetic measurements with the idea spec: an integrated diode emitter array spectrophotometer/fluorometer. *In* T Kuang, C Lu, L Zhang, eds, Photosynthesis for Food, Fuel and Future. Springer-Verlag, Beijing, pp 184–189

Heber U (2002) Irrungen, Wirrungen? The Mehler reaction in relation to cyclic electron transport in C3 plants. Photosynth Res **73:** 223–231

Joliot P, Johnson GN (2011) Regulation of cyclic and linear electron flow in higher plants. Proc Natl Acad Sci USA **108:** 13317–13322

Kanazawa A, Kramer DM (2002) *In vivo* modulation of nonphotochemical exciton quenching (NPQ) by regulation of the chloroplast ATP synthase. Proc Natl Acad Sci USA **99:** 12789–12794

Keeling CD, Bacastow RB, Bainbridge AE, Ekdahl CA, Guenther PR, Waterman LS, Chin JFS (1976) Atmospheric carbon dioxide variations at Mauna Loa Observatory, Hawaii. Tellus **28:** 538–551

Keys A, Bird I, Cornelius M (1978) Photorespiratory nitrogen cycle. Nature **275:** 741–743

Kramer D, Crofts A (1989) Activation of the chloroplast ATPase measured by the electrochronic change in leaves of intact plants. Biochim Biophys Acta **976:** 28–41

Kramer DM, Evans JR (2011) The importance of energy balance in improving photosynthetic productivity. Plant Physiol **155:** 70–78

Laisk A (1977) Kinetics of Photosynthesis and Photorespiration in C_3 Plants. Nauka, Moscow (in Russian)

Lea PJ, Miflin BJ (1974) Alternative route for nitrogen assimilation in higher plants. Nature **251:** 614–616

Lillo C, Appenroth KJ (2001) Light regulation of nitrate reductase in higher plants: which photoreceptors are involved? Plant Biol **3:** 455–465

Livingston AK, Cruz JA, Kohzuma K, Dhingra A, Kramer DM (2010) An *Arabidopsis* mutant with high cyclic electron flow around photosystem I (*hcef*) involving the NADPH dehydrogenase complex. Plant Cell **22:** 221–233

Loriaux SD, Avenson TJ, Welles JM, McDermitt DK, Eckles RD, Riensche B, Genty B (2013) Closing in on maximum yield of chlorophyll fluorescence using a single multiphase flash of sub-saturating intensity. Plant Cell Environ **36:** 1755–1770

Maxwell K, Johnson GN (2000) Chlorophyll fluorescence: a practical guide. J Exp Bot **51:** 659–668

Miflin BJ (1974) Nitrite reduction in leaves: studies on isolated chloroplasts. Planta **116:** 187–196

Miller AJ, Fan X, Orsel M, Smith SJ, Wells DM (2007) Nitrate transport and signalling. J Exp Bot **58:** 2297–2306

Miyake C, Miyata M, Shinzaki Y, Tomizawa K (2005) CO_2 response of cyclic electron flow around PSI (CEF-PSI) in tobacco leaves: relative electron fluxes through PSI and PSII determine the magnitude of non-photochemical quenching (NPQ) of Chl fluorescence. Plant Cell Physiol **46:** 629–637

Miyake C, Shinzaki Y, Miyata M, Tomizawa K (2004) Enhancement of cyclic electron flow around PSI at high light and its contribution to the induction of non-photochemical quenching of Chl fluorescence in intact leaves of tobacco plants. Plant Cell Physiol **45:** 1426–1433

Möhlmann T, Tjaden J, Schwöppe C, Winkler HH, Kampfenkel K, Neuhaus HE (1998) Occurrence of two plastidic ATP/ADP transporters in Arabidopsis thaliana L.: molecular characterisation and comparative structural analysis of similar ATP/ADP translocators from plastids and Rickettsia prowazekii. Eur J Biochem **252:** 353–359

Munekage Y, Hashimoto M, Miyake C, Tomizawa KI, Endo T, Tasaka M, Shikanai T (2004) Cyclic electron flow around photosystem I is essential for photosynthesis. Nature **429:** 579–582

Munekage Y, Hojo M, Meurer J, Endo T, Tasaka M, Shikanai T (2002) *PGR5* is involved in cyclic electron flow around photosystem I and is essential for photoprotection in *Arabidopsis*. Cell **110:** 361–371

Neuhaus HE, Thom E, Möhlmann T, Steup M, Kampfenkel K (1997) Characterization of a novel eukaryotic ATP/ADP translocator located in the plastid envelope of Arabidopsis thaliana L. Plant J **11:** 73–82

Noctor G, Foyer C (1998) A re-evaluation of the ATP:NADPH budget during C_3 photosynthesis: a contribution from nitrate assimilation and its associated respiratory activity? J Exp Bot **49:** 1895–1908

Noctor G, Foyer CH (2000) Homeostasis of adenylate status during photosynthesis in a fluctuating environment. J Exp Bot **51:** 347–356

Petersen J, Förster K, Turina P, Gräber P (2012) Comparison of the H^+/ATP ratios of the H^+-ATP synthases from yeast and from chloroplast. Proc Natl Acad Sci USA **109:** 11150–11155

Pilgrim ML, Caspar T, Quail PH, McClung CR (1993) Circadian and light-regulated expression of nitrate reductase in Arabidopsis. Plant Mol Biol **23:** 349–364

Rachmilevitch S, Cousins AB, Bloom AJ (2004) Nitrate assimilation in plant shoots depends on photorespiration. Proc Natl Acad Sci USA **101:** 11506–11510

Ruuska SA, Badger MR, Andrews TJ, von Caemmerer S (2000) Photosynthetic electron sinks in transgenic tobacco with reduced amounts of Rubisco: little evidence for significant Mehler reaction. J Exp Bot **51:** 357–368

Sacksteder CA, Kanazawa A, Jacoby ME, Kramer DM (2000) The proton to electron stoichiometry of steady-state photosynthesis in living plants: a proton-pumping Q cycle is continuously engaged. Proc Natl Acad Sci USA **97:** 14283–14288

Sacksteder CA, Kramer DM (2000) Dark-interval relaxation kinetics (DIRK) of absorbance changes as a quantitative probe of steady-state electron transfer. Photosynth Res **66:** 145–158

Scheibe R (2004) Malate valves to balance cellular energy supply. Physiol Plant **120:** 21–26

Seelert H, Poetsch A, Dencher NA, Engel A, Stahlberg H, Müller DJ (2000) Proton-powered turbine of a plant motor. Nature **405:** 418–419

Sharkey TD (1988) Estimating the rate of photorespiration in leaves. Physiol Plant **73:** 147–152

Shikanai T (2007) Cyclic electron transport around photosystem I: genetic approaches. Annu Rev Plant Biol **58:** 199–217

Smirnoff N, Stewart GR (1985) Nitrate assimilation and translocation by higher plants: comparative physiology and ecological consequences. Physiol Plant **64:** 133–140

Tazoe Y, von Caemmerer S, Estavillo GM, Evans JR (2011) Using tunable diode laser spectroscopy to measure carbon isotope discrimination and mesophyll conductance to CO_2 diffusion dynamically at different CO_2 concentrations. Plant Cell Environ **34:** 580–591

von Caemmerer S (2000) Biochemical Models of Leaf Photosynthesis, Vol 2. CSIRO, Collingwood, Australia

von Caemmerer S, Farquhar GD (1981) Some relationships between the biochemistry of photosynthesis and the gas exchange of leaves. Planta **153:** 376–387

Walker B, Ariza LS, Kaines S, Badger MR, Cousins AB (2013) Temperature response of in vivo Rubisco kinetics and mesophyll conductance in Arabidopsis thaliana: comparisons to Nicotiana tabacum. Plant Cell Environ **36:** 2108–2119